ELSEVIER

Journal of Nuclear Materials 277 (2000) 239–249

journal of nuclear materials

www.elsevier.nl/locate/jnucmat

Zirconia ceramics for excess weapons plutonium waste

W.L. Gong[a,*], W. Lutze[b], R.C. Ewing[c]

[a] *Center for Radioactive Waste Management, Advanced Materials Laboratory, University of New Mexico, 1001 University Blvd. SE, Albuquerque, NM 87106, USA*

[b] *Department of Chemical and Nuclear Engineering, University of New Mexico, Albuquerque, NM 87131, USA*

[c] *Department of Nuclear Engineering and Radiological Sciences, University of Michigan, Ann Arbor, MI 48109, USA*

Received 16 April 1999; accepted 15 July 1999

Abstract

We synthesized a zirconia (ZrO_2)-based single-phase ceramic containing simulated excess weapons plutonium waste. ZrO_2 has large solubility for other metallic oxides. More than 20 binary systems A_xO_y–ZrO_2 have been reported in the literature, including PuO_2, rare-earth oxides, and oxides of metals contained in weapons plutonium wastes. We show that significant amounts of gadolinium (neutron absorber) and yttrium (additional stabilizer of the cubic modification) can be dissolved in ZrO_2, together with plutonium (simulated by Ce^{4+}, U^{4+} or Th^{4+}) and impurities (e.g., Ca, Mg, Fe, Si). Sol–gel and powder methods were applied to make homogeneous, single-phase zirconia solid solutions. Pu waste impurities were completely dissolved in the solid solutions. In contrast to other phases, e.g., zirconolite and pyrochlore, zirconia is extremely radiation resistant and does not undergo amorphization. Baddeleyite (ZrO_2) is suggested as the natural analogue to study long-term radiation resistance and chemical durability of zirconia-based waste forms.

PACS: 81.05.Je; 81.20.-m; 81.30.-t; 61.10.Nz

1. Introduction

The directive resulting from the 1996 Moscow Summit between President Clinton and President Yelstin calls for surplus plutonium to be converted into forms that are resistant to reuse in nuclear weapons. The question is how to safely dispose of 100 tons of weapons grade plutonium declared surplus at the end of the Cold War. Additionally, there are impure chemical forms of plutonium that are also considered surplus.

It has been suggested to convert some forms of plutonium (Pu–Ga alloys and PuO_2) into mixed-oxide (MOX) fuel and to irradiate this fuel in commercial nuclear power reactors. In this way electrical energy would be generated and the remaining plutonium would be contained in discharged (spent) reactor fuel. In particular, it has been proposed that burning plutonium in a non-fertile fuel based on a zirconia matrix that may constitute a viable, final waste form [1,2]. Plutonium is believed to be sufficiently proliferation resistant because the spent non-fertile fuel is shielded by strong radiation. The deterrent provided by spent fuel is called the spent fuel standard [3]. The validity of the spent fuel standard as a barrier against fast and efficient recovery of plutonium can be questioned [4], since shortcuts have been published [5] and new ones are occasionally discovered [6].

Chemical forms of plutonium not appropriate for conversion into MOX require other methods of treatment and conversion into proliferation-resistant waste forms, suitable for storage and disposal. In the US, this inventory may be as high as 50 tons of plutonium. The waste forms currently under development are ceramics, though glasses have been studied as well [7]. If properly selected and manufactured, ceramic and vitreous host phases can accommodate the chemically impure forms of plutonium currently stored in weapons plutonium

* Corresponding author. Tel.: +1-505 272 7142; fax: +1-505 272 7304.

E-mail address: wgong@unm.edu (W.L. Gong).

0022-3115/00/$ - see front matter
PII: S0022-3115(99)00195-6

processing facilities. Generally, ceramic forms are chemically far more durable than vitreous waste forms, particularly at higher temperatures or in flowing water [8]. There are chemically durable and radiation-resistant minerals, e.g., baddeleyite (ZrO_2) that form solid solutions with plutonium oxide and are candidate waste forms for interim storage and disposal of pure plutonium [9], should the option of re-use as MOX fuel not be pursued. Radiation resistance is important, because the waste form is expected to confine fissile material, ^{239}Pu (2.43×10^5 yr Half-life) and its daughter ^{235}U ($t_{1/2}=7\times10^8$ yr) for a very long time.

Glass and ceramic waste forms can provide proliferation resistance comparable to that of spent fuel. There are approaches to development of such waste forms, as the following examples show:

1. A can-in-can concept, where the Pu waste form (ceramic or glass) is embedded in vitrified high-level radioactive waste.
2. If ceramic or glass waste forms are not embedded in vitrified high-level radioactive waste, an equivalent radiation field can be provided by a admixture of ^{137}Cs. There is plenty of ^{137}Cs in storage in the US. Between 10 and 300 yr after discharge of the fuel from the reactor, ^{137}Cs determines the dose rate of spent fuel and of vitrified high-level waste.
3. Plutonium could be burnt in non-fertile reactor fuel, where UO_2 is replaced by another ceramic such as ZrO_2 or $MgAl_2O_4$. Calculations have shown that over 93% of the fissile plutonium can be burnt [10]. The spent non-fertile fuel would meet the spent fuel standard.
4. A chemical method to discourage extraction of plutonium would be to make solid solutions of plutonium and thorium oxides. Dissolution of such systems is extremely slow [11].
5. Plutonium could be disposed of in deep boreholes without a radiation shield [3].

The most promising mineral host phases for Pu include apatite, pyrochlore, zirconolite, monazite, zircon and zirconia. The physical and chemical properties of these minerals, except zirconia, were reviewed recently by Ewing et al. [12].

A pyrochlore/zirconolite ceramic, containing other phases such as brannerite, actinide oxides and rutile, has been selected for plutonium wastes in the US [13] and is currently under development at Lawrence Livermore National Laboratory. Pyrochlore is a derivative of the fluorite structure type. In the general formula $A_2B_2X_6Y$ larger cations are in the A-site such as Na, Ca, U, Th, Y, and rare-earth elements (REE), and smaller, high-valent cations preferably in the B-site (Nb, Ta, Ti, Zr, Fe^{3+}). Zirconolite ($CaZrTi_2O_7$) is one of the three main phases in Synroc, the most extensively studied ceramic waste form for high-level radioactive waste [8]. Monoclinic zirconolite is a fluorite-derivative structure closely related to pyrochlore. Zirconolite is the primary actinide host in Synroc with the actinides accommodated in the A-site. Pu incorporation into zirconolite has been studied [14,15]. The pyrochlore phase $Gd_2Ti_2O_7$ has been extensively studied in terms of radiation damage [16,17] as was shown to become fully amorphous at a dose of 3.1×10^{18} α-decay events/g. The crystalline-to-amorphous transition is accompanied by a factor of 50 decrease in chemical durability. Amorphization induced by alpha-decay events in zirconolite has been observed for and ^{244}Cm-doped [16] and ^{238}Pu-substituted [16,18,19]. Pyrochlores occur naturally with up to 30 wt% of uranium in the A-site. Natural occurrences of zirconolite are rare, but samples have been studied extensively [17,20–22]. Both minerals are often found to be metamict with chemical alterations in nature [23–26]. Zirconolite is less susceptible to radiation-induced amorphization than is pyrochlore [27].

Usually, multi-phase ceramics are easier to make than are single-phase ceramics, if a wide range of waste constituents must be accommodated in solid solutions. Even in multi-phase ceramics, small amounts of waste constituents may concentrate in minor additional phases, sometimes as a silicate glass [7,13]. In the multi-phase pyrochlore/zirconolite ceramic waste form for plutonium waste, plutonium and neutron absorbers (e.g., Hf and Gd), as well as waste impurities (e.g., U, Ca, Mg, Fe) enter different crystalline hosts according to their individual crystallochemical behaviors. The Gd is partitioned preferentially into the pyrochlore phase and Hf into the zirconolite phase. U and Pu may also separate into different phases, e.g., actinide oxide phases. Heterogeneous partitioning and phase separation may cause a decrease in chemical durability.

The objective of this investigation is to study the ternary system ZrO_2–MO_2–REE_2O_3 and to find a field of compositions for single-phased ceramics of cubic structure with excess weapons plutonium wastes. M stands for Pu, U and Th. We simulate plutonium by cerium. Uranium is the decay product of plutonium and may also be a waste component initially. Thorium may be included in the waste form and will complicate extraction of plutonium. REE_2O_3 includes Gd_2O_3 as a neutron absorber to prevent criticality and Y_2O_3 as a stabilizer of the cubic modification of ZrO_2.

2. Zirconia

Zirconia, ZrO_2, occurs in nature in its monoclinic modification as the mineral baddeleyite. Structural transformation from monoclinic to tetragonal takes place at 1170°C and from tetragonal to cubic at 2370°C. This modification is stable between 2370°C and the melting point at 2680°C [28]. In the cubic modification, the cations are arranged in a face-centered lattice (fluo-

rite-type structure). Cubic ZrO_2 can be stabilized by tetravalent cations in ZrO_2–MO_2 systems, where $M = Ce^{4+}$, Th^{4+}, U^{4+} [29, 30]. Stabilization can also be achieved by oxygen vacancies introduced by trivalent cations such as rare-earth oxides REE_2O_3 [31] and by divalent cations such as CaO and MgO. Zirconium in ZrO_2 can be substituted by many other metals without changing the crystal structure.

2.1. Solid solutions

Table 1 lists zirconia solid solution systems relevant to excess weapons Pu wastes [32–48]. Typical impurity oxides in these Pu wastes include UO_2, Al_2O_3, MgO, Ga_2O_3, Fe_2O_3, Cr_2O_3, NiO, MoO_2, SiO_2, WO_2 and ZnO [13]. Table 1 shows that there is substantial solid solubility of ZrO_2 for many of these oxides. There is complete miscibility in the ZrO_2–PuO_2 system. Other oxides that form solid solutions with zirconia are SrO, CdO, CoO, MnO, Bi_2O_3, Sb_2O_3, Sc_2O_3, In_2O_3, Nb_2O_5, Ta_2O_5, TiO_2, GeO_2, VO_2 and SnO_2. Miscibility gaps can be decreased by adding Y_2O_3 or other stabilizers. For example, a much larger solubility of Nb^{5+}or Ta^{5+}can be obtained by doping ZrO_2 with a divalent or trivalent cation, as shown by Prietzel et al. [49] for the system ZrO_2–MgO–Ta_2O_5 and by Kim and Tien [50] for the system ZrO_2–Y_2O_3–Ta_2O_5.

2.2. Radiation effects

Naguib and Kelly's review of literature data on radiation damage in zirconia shows high stability of this refractory oxide against amorphization [51]. Ion irradiation studies did not show amorphization in yttrium-stabilized zirconia up to high doses [52–56]. For instance, no amorphization was observed after irradiation with 400 keV Xe^+ ions up to a dose of 110 displacement per atom (dpa) at 90°C [57] and after irradiation of ZrO_2 with 240 keV Xe^+ ions at room temperature up to about 200 dpa [52]. In two studies, a cubic zirconia solid solution $(Zr_{0.75}Th_{0.10}Y_{0.10}Er_{0.05})O_{1.925}$ was irradiated with 1.5 MeV Xe^+ ions up to 25 dpa at −253°C. Electron diffraction showed that the bulk of the sample remained crystalline [56,58]. For comparison, zircon, $ZrSiO_4$ becomes completely amorphous at 0.3 dpa under the same experimental conditions [59]. Comparing the data on radiation damage in the reviews in [12] and [60] with ZrO_2 shows that ZrO_2 is by far the most radiation resistant ceramic host phase.

2.3. Natural analogues

The mineral baddeleyite (ZrO_2) occurs in many terrestrial and lunar samples and in some achondrites as a trace constituent. Baddeleyite crystallizes from chemically fractionated mafic magmas together with apatite, ilmenite, zircon and zirconolite. Baddeleyite forms in tektites as a dissociation product of zircon during meteorite impact. It is also found as rims on mantle zircon megacrysts in kimberlites [61]. Baddeleyite is a major carrier of Hf, Ti, Fe, Nb, Y and W (Table 2) and contains up to 3000 ppm U or Th [62–67]. The high U content and the lack of any chemical alteration in geological processes, i.e., negligible or no Pb loss are indicative of high chemical durability and explain the rapidly growing number of publications on U–Pb baddeleyite dating. Emplacement ages with unprecedented accuracy have been obtained with baddeleyite for many Precambrian mafic and alkaline rocks that experienced geological processes 544–2500 million years ago [61]. Baddeleyite provides an excellent suite of natural samples to evaluate the chemical durability and radiation

Table 1
Solid solutions in binary systems with ZrO_2 (in mol%)

Binary system	Solubility limit	Ref.	Binary system	Solubility limit	Ref.
ZrO_2–PuO_2	100	[32]	ZrO_2–Fe_2O_3	40	[41]
ZrO_2–UO_2	[a]	[33]	ZrO_2–Cr_2O_3	11	[42]
ZrO_2–ThO_2	[a]	[34]	ZrO_2–Ga_2O_3	33	[43]
ZrO_2–REE_2O_3	25–80[b]	[35]	ZrO_2–CaO	24	[44]
ZrO_2–CeO_2	20	[36]	ZrO_2–MgO	30	[44]
ZrO_2–HfO_2	100		ZrO_2–NiO	10	[45]
ZrO_2–WO_2	12	[37]	ZrO_2–ZnO	60 wt%	[46]
ZrO_2–SiO_2	10	[38]	ZrO_2–PbO	50	[47]
ZrO_2–RuO_2	13	[39]	ZrO_2–Na_2O	3 wt%	[48]
ZrO_2–Al_2O_3	40	[40]			

[a] Two solid solutions: $(ZrO_2)_{ss}$ and $(MO_2)_{ss}$ with little mutual solubility (M = U or Th).

[b] The solubility limit for rare-earth oxides in ZrO_2 depends on their ion-radii. Roughly the solubility limit for a rare-earth element increases with decrease of its radius. Yb_2O_3 has higher solubility limit, ~ 80 mol% in ZrO_2 with fluorite structure as Yb^{3+}ion is very small in size, 0.0868 nm ($CN = 6$). However, La_2O_3 has lower solubility, ~ 25 mol% as La^{3+}ion is very large in size, 0.1032 nm ($CN = 6$).

Table 2
Geochemical composition of baddeleyite from various rock types (wt%)

Sample	1	2	3	4	5	6	7	8
ZrO_2	97.49	92.59	90.63	95.2	87.25	93.49	92.13	95.52
FeO	0.36	2.15	0.63	0.39	0.80	1.22	0.49	0.20
TiO_2	1.06	2.52	6.10	2.51	7.93	2.94	–	0.14
CaO	0.03	–	0.65	0.06	0.53	0.12	0.25	0.05
MgO	–	0.21	0.09	0.08	0.10	0.09	–	0.06
MnO	0.04	0.09	0.05	0.05	0.16	0.17	–	0.05
SiO_2	0.01	0.34	–	–	0.21	0.29	0.68	–
Al_2O_3	0.01	0.18	0.11	0.03	0.15	0.12	0.27	–
HfO_2	0.96	1.30	–	2.19	–	–	1.27	1.62
Cr_2O_3	0.03	0.17	0.11	0.04	0.27	0.14	–	–
Y_2O_3	0.28	–	–	–	1.27	1.47	–	–
Nb_2O_5	–	–	–	–	1.03	0.65	WO_3/3.06	Ta_2O_5/0.42
Total	100.27	99.55	98.37	100.54	99.70	100.70	98.15	100.20
Ref.	[62]	[63]	[64]	[61]	[65]	[65]	[66]	[67]

stability of Pu loaded zirconia ceramics for over long periods of geological time much longer than the half-life of ^{239}Pu and comparable with that of ^{235}U.

Baddeleyite occurs in heavy mineral concentrates of streams and persists in these placer deposits because of its high chemical and mechanical durability [68] Thermodynamic calculations showed that zirconia has a very low solubility, $<10^{-10}$ mol/L with little temperature or flow rate dependence [69]. Leaching studied were performed to estimate the chemical durability of cubic zirconia (9.4 mol% Y_2O_3) in a nuclear waste disposal site in granitic rock. The leaching rate in saline groundwater at a temperature of 85°C was 5.8×10^{-4} gm^{-2} d^{-1} [70].

3. Experimental

Zirconia solid solutions were prepared by reaction sintering of cold-pressed powders at temperatures between 1400°C and 1600°C. Powders were obtained either by grinding and mixing the respective metal oxides or by a sol–gel process. The solid solution compositions are listed in Table 3.

Powder method: The starting materials were powders of oxides: ZrO_2, CeO_2, Gd_2O_3, Y_2O_3, MgO, CaO, Fe_2O_3 and SiO_2. All chemicals were analytical grade. Oxides in desired molar ratios (Table 3, samples #1–4) were mixed and ground in acetone in a ball mill. After drying, powders were cold pressed into pellets at 80 MPa and sintered in air at 1100°C for 6 h. These samples were then transferred to a high-temperature furnace and sintered in air for another 6 h at 1600°C.

Sol–gel method: The starting materials were used as nitrates [$ZrO(NO_3)_2{\cdot}2H_2O$, $UO_2(NO_3)_2{\cdot}6H_2O$, $Gd(NO_3)_3{\cdot}6H_2O$, $Mg(NO_3)_2$, $Ca(NO_3)_2$, $Fe(NO_3)_3$, $Y(NO_3)_3{\cdot}6H_2O$], chloride [$ThCl_4{\cdot}4H_2O$] and Si as tetraethoxysilane [$Si(OC_2H_5)_4$]. Mixtures of salts in desired molar proportions (Table 3, samples #5–9) were dissolved in dilute nitric acid. Tetraethoxysilane was dissolved in methanol–water. Then, 10 mol% NH_4OH

Table 3
Nominal compositions of zirconia solid solutions and experimental summary

#	Stoichiometry[a]	Method	Temperature (°C)	Structure	a_0 (nm)
1	$Zr_{0.61}Gd_{0.26}Ce_{0.13-x}O_{1.87}$	Powder	1600	fcc, fluorite type	0.538
2	$Zr_{0.68}Gd_{0.18}Ce_{0.14-x}O_{1.91}$	Powder	1600	fcc, fluorite type	
3	$Zr_{0.61}Gd_{0.17}Ce_{0.13-x}Y_{0.09}O_{1.87}$	Powder	1600	fcc, fluorite type	0.520
4	$Zr_{0.57}Gd_{0.17}Ce_{0.17-x}Y_{0.09}O_{1.87}$	Powder	1600	fcc, fluorite type	0.521
5	$Zr_{0.70}Gd_{0.15}U_{0.15}O_{1.925}$	Sol–gel	1400	fcc, fluorite type	0.535
6	$Zr_{0.75}Gd_{0.15}Th_{0.10}O_{1.925}$	Sol–gel	1500	fcc, fluorite type	0.536
7	$Zr_{0.70}Gd_{0.15}Th_{0.15}O_{1.925}$	Sol–gel	1400	fcc, fluorite type two phases	$a_1 = 0.519$; $a_2 = 0.558$
			1500	fcc, fluorite type two phases	$a_1 = 0.532$; $a_2 = 0.565$
8	$Zr_{0.70}Gd_{0.15}Th_{0.15-x}O_{1.925}$	Sol–gel	1400	fcc, fluorite type two phases	
9	$Zr_{0.57}Gd_{0.15}Th_{0.13}Y_{0.15}O_{1.85}$	Sol–gel	1400	fcc, fluorite type two phases	0.538
			1500	fcc, fluorite type one phase	0.538

[a] x in the formulae represents Ca + Mg + Fe + Si ≈ 2 mol%. a_1 is for Th-poor $(ZrO_2)_{ss}$ and a_2 for Th-rich $(ZrO_2)_{ss}$.

solution was added slowly to the vigorously stirred mixture producing a white gel. These resulting gels were washed three times with absolute methanol to remove chloride. The gels were dried at 120°C, then ground and calcined at 800°C, milled and then cold-pressed at 80 MPa into cylindrical pellets (3 cm in diameter, 1 cm high). The pellets were fired at 1400°C or 1500°C in air for 6 h (some up to 36 h).

The synthesized ceramic materials were characterized with the help of analytical electron microscopy (AEM). Two transmission electron microscopes, JEM 2010 and 2000FX, were used and operated at 200 keV. The JEM 2010 was equipped with a Link ISIS and the 2000 FX with a TN-5500 system for energy dispersive X-ray emission spectroscopy (EDS). We conducted qualitative and quantitative analyses to determine chemical compositions of the phases observed. Bright-field imaging (BF) was used to characterize the microstructure of the ceramics. Selected area electron diffraction (SAED) was used to identify the crystal structure of individual phases. Analytical scanning electron microscopy was performed on a JEOL 5800lv microscope (20 keV electron beam). X-ray powder diffraction (XRD) analyses were performed using a Rigaku Denki diffractometer and CuKα radiation. Semi-quantitative calculations of phase concentrations were completed using Jade software.

4. Results

In Table 3 we list our zirconia solid solution compositions, methods and temperatures of preparation, the number of phases, and structural information. Cerium doped samples (#1–4 in Table 3) were prepared by reaction sintering of oxide powder mixtures at 1600°C. All other samples were prepared by the sol–gel method. The temperatures for reaction sintering of powders derived from the sol–gel process were 1400°C and/or 1500°C. The second last column of Table 3 shows that all solid solutions are of the fluorite structure type. Lattice constants a_0 are given in the last column. The ceramics are single phased, except samples #7–9 (1400°C). Samples #1–4 and sample #8 contain 2 mol% impurities (Ca, Mg, Fe and Si). These represent constituents encountered in excess weapons plutonium wastes.

Fig. 1(a) shows an EDS spectrum typical of a Ce-doped $(ZrO_2)_{ss}$ ceramic (sample #2, Table 3). Impurities are homogeneously dissolved in the ZrO_2 host structure. Peak intensities are constant throughout the sample. Fig. 1(b) shows an electron backscattering image of the same sample. The inset is an SAED pattern showing that the structure is cubic (fluorite type). The grain size of this ceramic ranges between 10 and 40 μm. Fig. 2 shows XRD patterns of Ce-doped $(ZrO_2)_{ss}$ ceramics (samples #1, 3 and 4). There is a small decrease in the lattice

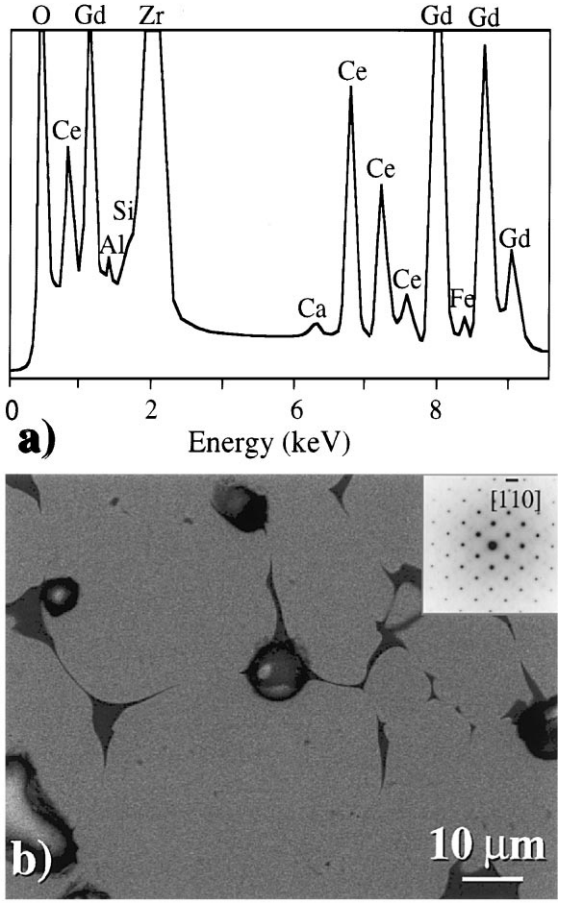

Fig. 1. Data on a chemically homogeneous, single-phase Ce-doped $(ZrO_2)_{ss}$ ceramic. The ceramic, with a nominal composition $Zr_{0.61}Gd_{0.26}Ce_{0.13-x}O_{1.87}$ ($X = Ca + Mg + Fe + Si = 2$ mol%), was sintered at 1600°C for 6 h. (a) EDS pattern; Peaks for Si, Ca and Fe are visible. The peak for Mg is overlapped by that for Gd. (b) Backscattered electron image. The inset is an SEAD pattern showing that the crystal is cubic with fluorite structure.

constant when the concentration of Gd is lowered, comparing samples #1 and 3. The diffraction patterns were generated by one phase, $(ZrO_2)_{ss}$, with different chemical compositions. Fig. 3(a) shows the XRD pattern of a U-doped $(ZrO_2)_{ss}$ ceramic (sample #5, Table 3). This ceramic and the ones to be described hereafter (samples #6–9) were produced by a sol–gel process. The grain size of these ceramics is much smaller (<1 μm), see Figs. 4, 5 and 7, than that seen in Fig. 1(b). Fig. 3(b) shows the XRD pattern of sample #7 (Table 3). There are two ZrO_2 solid solutions. One phase has a smaller cubic unit cell ($a_0 = 0.519$ nm) than the other ($a_0 = 0.558$ nm). The phase with the smaller unit cell contains ~ 8 mol% thorium ($Zr_{0.74}Gd_{0.18}Th_{0.08}O_{1.91}$) and constitutes about 70 wt% of the ceramic. The other phase contains

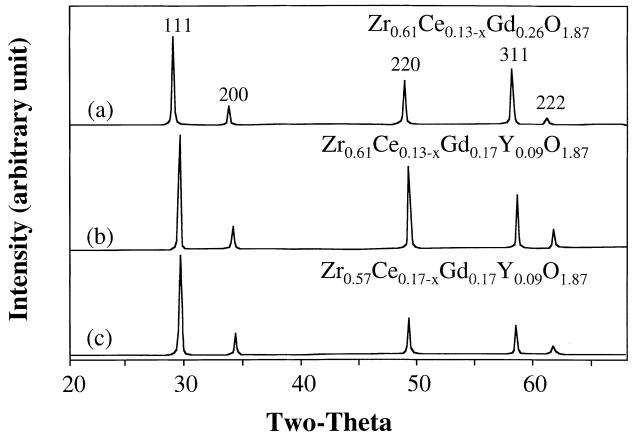

Fig. 2. XRD patterns of single phase, Ce-doped cubic $(ZrO_2)_{SS}$. All the solid solutions are the fluorite structure type. X = Ca + Mg + Fe + Si = 2 mol%.

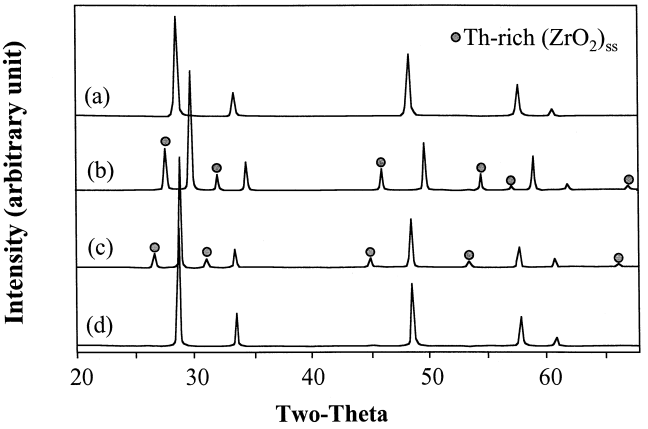

Fig. 3. XRD patterns of $(ZrO_2)_{SS}$ ceramics containing Th. (a) The ceramic with a nominal composition $Zr_{0.70}Gd_{0.15}U_{0.15}O_{1.925}$ (#5, Table 3) sintered at 1500°C. Only one single phase, cubic zirconia solid solution with fluorite structure is present. (b) The ceramic with a nominal composition $Zr_{0.70}Gd_{0.15}Th_{0.15}O_{1.925}$ (#7, Table 3) sintered at 1400°C. Two zirconia solid solutions are present. Filled circles mark the peaks belonging to the Th-rich $(ZrO_2)_{SS}$. The other peaks belong to the Th-poor $(ZrO_2)_{SS}$. (c) The ceramic with the same nominal composition (#7, Table 3) but sintered at 1500°C. The Th-rich $(ZrO_2)_{SS}$ phase still exists but with a reduced concentration (~ 15 wt%). Filled circles mark the peaks belonging to the Th-rich $(ZrO_2)_{SS}$. The other peaks belong to the Th-poor $(ZrO_2)_{SS}$. (d) The ceramic with a nominal composition $Zr_{0.70}Gd_{0.15}Th_{0.10}O_{1.925}$ (#6, Table 3) sintered at 1500°C. Only a single phase, cubic zirconia solid solution with fluorite structure type is present.

~ 30 mol% thorium ($Zr_{0.60}Gd_{0.10}Th_{0.30}O_{1.95}$). Concentrations were measured by AEM. Fig. 4 is a TEM bright field image showing the two phases. The grain size of the dark Th-rich phase varies between 20 and 100 nm. The other phase is more uniform in size with an average of 500 nm. SAED analyses were conducted to obtain structural information from different crystalline grains. The results are consistent with those from XRD analyses of powders. Also, we did not detect any other phases of low total yield in the TEM images that may not have been detected by XRD. Hence, there are only two cubic phases.

Increasing the reaction sintering temperature of sample #7 from 1400°C to 1500°C yielded still a phase separated ceramic but decreased the mass fraction of the Th-rich phase from 30% to 15%. The XRD pattern in Fig. 3(c) shows the change in the yields. The unit cell for the Th-rich $(ZrO_2)_{ss}$ was increased to $a_0 = 0.565$ nm and that for Th-poor $(ZrO_2)_{ss}$ was increased to $a_0 = 0.532$ nm). The unit cell increase for Th-poor $(ZrO_2)_{ss}$ was due to ThO_2 dissolution into ZrO_2 enhanced at higher temperature. Fig. 3(d) shows that a single-phase ceramic was obtained at 1500°C by lowering the thorium concentration from 15 to 10 mol%, at constant gadolinium concentration.

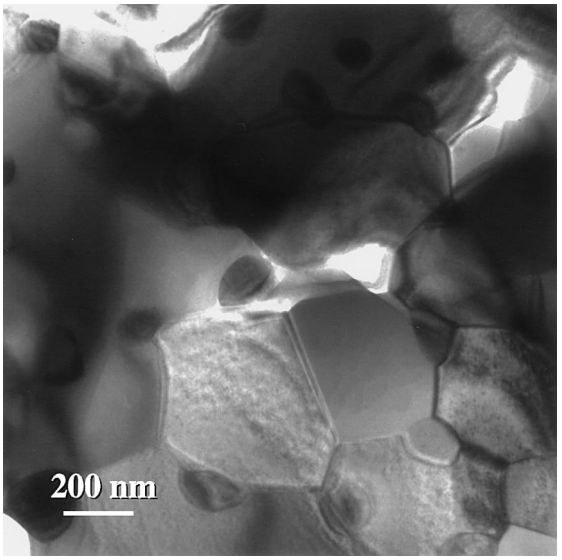

Fig. 4. TEM bright field image showing the microstructure of a phase separated $(ZrO_2)_{SS}$ ceramic. The ceramic with a nominal composition $Zr_{0.70}Gd_{0.15}Th_{0.15}O_{1.925}$ sintered at 1400°C. Small black particles are richer in ThO_2 than brighter, larger crystals.

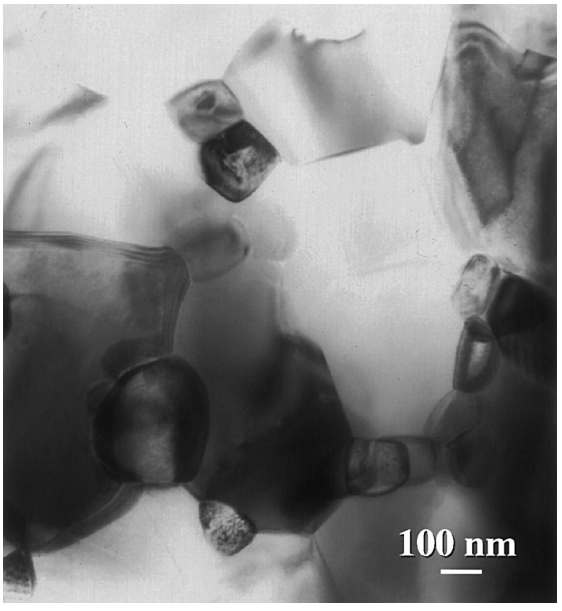

Fig. 5. TEM bright field image showing the microstructure of a phase-separated $(ZrO_2)_{SS}$ ceramic. The ceramic with a nominal composition $Zr_{0.70}Gd_{0.15}Th_{0.15-x}O_{1.925}$ (X = Ca + Mg + Fe + Si = 2 mol%) sintered at 1400°C. Small black particles are richer in ThO_2 than brighter, larger crystals.

Fig. 5 is a bright field image showing the microstructure of ceramic sample #8 (Table 3). In this sample, the thorium concentration was lowered from 15 mol% (sample #7) to 13 mol% and impurities (Ca, Mg, Fe, Si) were added ($x = 2$ mol%). Reaction sintering was completed at 1400°C. As with sample #7, a two-phase ceramic was obtained. The small dark crystals are enriched in thorium relative to the larger and lighter ones. The TEM samples were carefully searched for minor phases with a composition different from the two solid solutions but nothing was found. EDS analyses showed that the impurities are homogeneously distributed throughout the ceramic.

Fig. 6 shows XRD patterns of ceramic #9 (Table 3). In this sample, we added 15 mol% Y_2O_3. The Gd_2O_3 and ThO_2 concentrations are the same as in sample #8. No impurities were added. Reaction sintering at 1400°C yielded the same results as obtained with samples #7 and 8 at 1400°C. Ceramic #8 is a two-phase ceramic with two ZrO_2 solid solutions of cubic structure. Ceramic #9 consists of two solid solutions with different ThO_2 concentrations Fig. 6(a). Again, the phase with the higher thorium content shows the lower yield and the crystals are smaller in size. Synthesis of ceramic #9 at 1500°C shows an effect of yttrium on the solubility of thorium, if we compare Fig. 6(a) with Fig. 3(b). The XRD pattern in Fig. 6(b) shows essentially one phase. A trace of a second phase may be visible at low diffraction angles. Fig. 7 is a TEM bright field image showing ceramic #9 sintered at 1500°C. Assessment of this sample shows that yttrium enhances the solubility of thorium oxide in zirconium oxide.

5. Discussion

Concentrations of 1 to 10 wt% in excess weapons plutonium waste forms are under consideration [13,71]. In these studies, We took 15 mol% as an upper limit of MO_2 and 26 mol% as an upper limit of REE_2O_3.

Between 1400°C and 1600°C, our temperature range for ceramic syntheses, pure ZrO_2 is stable in its tetragonal modification. Depending on their concentrations, many compounds, including rare-earth oxides (Table 1), form single-phase solid solutions with ZrO_2 at 1400°C, stabilizing zirconia's cubic or tetragonal modification. No changes in modification are observed upon cooling to room temperature.

Making a waste form with fissile materials such as ^{239}Pu requires selection and incorporation of special components to avoid criticality. In the event of contact of the waste form with water, e.g., in the repository, there should be no or only a negligible effect on neutron moderation and reflection, i.e., the waste form should be overmoderated. This can be effected by an absorber for thermal neutrons that becomes part of the ZrO_2 solid solution. The ceramic solid solution is then intimately mixed with a moderator material and sintered by hot uniaxial pressing.

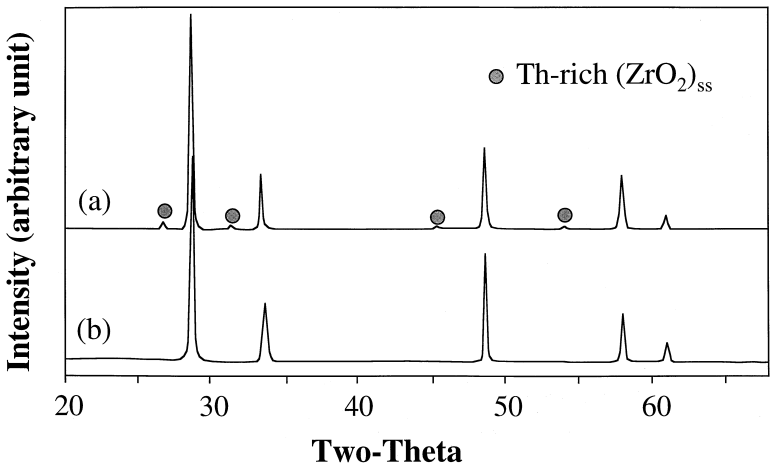

Fig. 6. XRD patterns of $(ZrO_2)_{SS}$ ceramics showing the effect of yttrium addition and temperature increase. (a) The ceramic with a nominal composition $Zr_{0.57}Gd_{0.15}Th_{0.13}Y_{0.15}O_{1.85}$ (#9, Table 3) sintered at 1400°C. Two zirconia solid solutions exist but Th-poor $(ZrO_2)_{SS}$ is dominant in volume as compared to Figs. 3(b) and 3(c). Filled circles mark the peaks belonging to the Th-rich $(ZrO_2)_{SS}$. (b) The ceramic with the same nominal composition (#9, Table 3) but sintered at 1500°C. Here only a single phase, cubic zirconia solid solution with fluorite structure type is present.

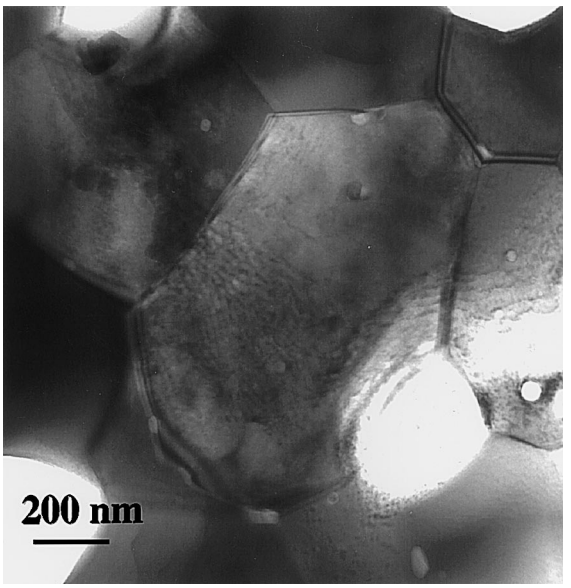

Fig. 7. TEM bright field image showing the microstructure of a single-phase, cubic $(ZrO_2)_{SS}$ ceramic with Th simulating Pu. The ceramic has a nominal composition $Zr_{0.57}Gd_{0.15}Th_{0.13}Y_{0.15}O_{1.85}$ (#9, Table 3) and was sintered at 1500°C. Small black particles rich in ThO_2 are seldom observed.

To make a ceramic waste form for plutonium, we added rare-earth elements to provide for capture of thermalized neutrons. In this regard, gadolinium is the most efficient rare-earth element. It has the highest known absorption cross-section for thermal neutrons of all metals. The solubility of Gd_2O_3 in ZrO_2 is high (60 mol%) [72]. A minimum concentration of ~ 8 mol% Gd_2O_3 is necessary [70] to obtain a cubic solid solution with fluorite structure. For Y_2O_3 the corresponding value is ~ 7 mol% [35]. Y_2O_3 is one of the stabilizers used in commercial ZrO_2 ceramics. We conducted experiments with both rare-earth oxides (Table 3). Moderators such as BeO or $BeSiO_4$ were briefly mentioned by the authors in a recent paper [73]. Meanwhile, we conducted criticality calculations to study this effect quantitatively. As an example, a $(ZrO_2)_{ss}$ with 10 at.% Pu and 12–18 at.% Gd can provide a moderated system with little effect on K_{eff} from an infinite amount of water. In the calculations, boehmite, AlO(OH) acts as a moderator. The details of this work will be reported separately [84].

Addition of 15 mol% PuO_2 to a $85ZrO_2$–$15Gd_2O_3$ solid solution would yield a ternary solid solution with fluorite structure. Above 1000°C, ZrO_2 and PuO_2 form cubic solid solutions in the complete range of composition, except at Pu concentrations <5 mol% [32]. The solubility of Pu in ZrO_2 is 100% (Table 1). PuO_2 is an effective stabilizer for cubic zirconia, and so is gadolinium. Recent experiments showed that a zirconia solid solution with 20.9 wt% Gd_2O_3 and 10.3 wt% PuO_2 is a single phase solid solution of cubic structure [74]. We selected CeO_2 to simulate PuO_2.

There is complete miscibility within the binary systems of ZrO_2–PuO_2, CeO_2–PuO_2 [75], UO_2–PuO_2 [76] and ThO_2–PuO_2 [77]. All structures are cubic (fluorite type). In ZrO_2, the solubility decreases with increasing ionic radius of the substituting atom from Pu (100 mol%), CeO_2 (20 mol%), UO_2 (~ 3 mol%) to ThO_2 (~ 2 mol%). The structures are tetragonal for all elements

with limited solubility (Ce, U, Th). The ionic radii for a coordination number of 8 are: $Pu^{4+} = 0.096$, $Ce^{4+} = 0.097$, $U^{4+} = 0.10$ and $Th^{4+} = 0.105$ (nm) [78], suggesting that Ce^{4+} is the best substitute for Pu^{4+}, followed by U^{4+} and Th^{4+}.

We synthesized four ceramics with CeO_2 (samples #14, Table 3). We studied the effect of gadolinium, yttrium, and waste constituents on phase stability, composition and crystal structure. A total of 2 mol% MgO, CaO, Fe_2O_3 and SiO_2 was added to represent excess weapons plutonium waste impurities. Samples #1 and 2 contain 11(26) and 12(18) mol% Ce(Gd), respectively, and are cubic. Samples #3 and 4 contain 11(17 + 9) and 15(17 + 9) mol% Ce(Gd + Y), respectively. All ceramics are single-phased and cubic (fluorite type). Impurities were found to be homogeneously distributed within the solid solution Fig. 1(a). With 1600°C as the temperature for reaction sintering, the dry route (powder technology) could be applied to make a waste form for plutonium, using commercially available oxides.

Long-term phase stability of a $(ZrO_2)_{ss}$ may be affected by transmutation. Within 5×10^4 yr, 75% of plutonium decays into uranium. The solubility of UO_2 in ZrO_2 is very limited. The phase diagram and thermodynamic properties of ZrO_2–UO_2 were studied by various investigators [79–83]. The binary system consists almost entirely of $(ZrO_2)_{ss}$ and $(UO_2)_{ss}$ with low solubility on either side of the miscibility gap. Between 1100°C and 1700°C in air, the zirconia phase $(ZrO_2)_{ss}$ is tetragonal. No experimental information is available on the effect of transmutation. However, a system ZrO_2–PuO_2–UO_2 in which uranium is successively substituted for plutonium may become thermodynamically unstable and is expected to undergo phase separation.

Sample #5 in Table 3 is similar in composition to sample #2 but contains 15 mol% UO_2 instead of 12 mol% CeO_2. Our results show that the effect of gadolinium in our ZrO_2–Gd_2O_3–UO_2 system is twofold: it increases the solubility of uranium in ZrO_2 and renders the cubic rather than the tetragonal modification of ZrO_2 stable. A single-phase ceramic with 15 mol% UO_2 formed at 1400°C. The structure is the same as for the binary ZrO_2–Gd_2O_3 solid solution (fluorite type).

In the system ZrO_2–ThO_2, two solid solutions, tetragonal $(ZrO_2)_{ss}$ and cubic $(ThO_2)_{ss}$, exist at 1000–2000°C [34]. The mutual solubility in the end-members is about 2 mol%. We synthesized four samples (#6–9, Table 3). Sample #7 compares directly with sample #5. Sample #7 contains 15 mol% ThO_2 instead of UO_2. Sample #6 contains only 10 mol% ThO_2. As with uranium, the effect of gadolinium is that it increases the solubility of thorium in ZrO_2 but not quite as much. At 10 mol% of ThO_2 and a ratio of $REE_2O_3/MO_2 = 1.5$, a single-phase ceramic is obtained. A single-phase cubic $(ZrO_2)_{ss}$ was also reported for the composition $Zr_{0.75}Y_{0.10}Er_{0.5}Th_{0.10}O_{1.925}$ [56]. Here the ratio is also 1.5. At 15 mol% ThO_2, two phases formed with different yields and largely different concentrations of thorium (see Section 4). The effect of gadolinium on the crystal structure of the solid solution was the same as in sample #5 (Table 3). All solid solutions with thorium were cubic (fluorite type). Sample #8 with 13 mol% ThO_2 and impurities added is a small variation of sample #7. With 13 mol% ThO_2 the solubility of thorium in ZrO_2 is still exceeded. The solubility S is obviously in the range $10 < S < 13$ mol%. Addition of 15 mol% Y_2O_3 to the 15 mol% Gd_2O_3 does not have a dramatic effect on S. The microstructure of sample #9 shows that there is less phase separation at 1400°C than in samples #7 and 8. An increase of the reaction sintering temperature to 1500°C eliminated the second phase almost completely. The effect of increased temperature on S was less than with sample #7.

The fact that ceramics #7 and 8 contain two ZrO_2 dominated solid solutions may be explained by slow reaction kinetics and the compositions may not reflect equilibrium compositions. This was not further investigated. In the early stages of reaction there may have been a $(ThO_2)_{ss}$ and a $(ZrO_2)_{ss}$ with the $(ThO_2)_{ss}$ being unstable in the presence of REE_2O_3. The decrease in yield of the $(ThO_2)_{ss}$ with increased temperature and reaction time supports this assumption.

The results of our study are summarized in Fig. 8. The partial phase diagram of ZrO_2–MO_2–REE_2O_3 shows the phases and their structures as obtained at 1400–1600°C. The size of the gray region is tentative,

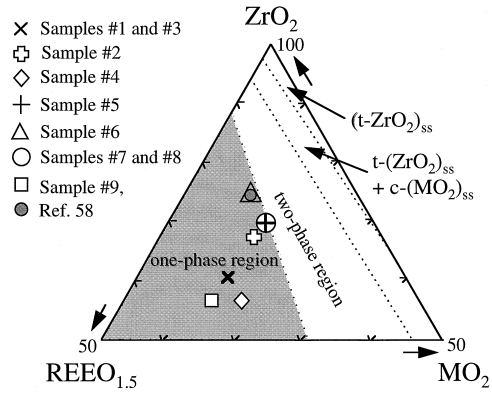

Fig. 8. Tentative phase relations of the ternary ZrO_2–REE_2O_3–MO_2 system at 1400–1600°C. The sample compositions are listed in Table 3. The zirconia sample from Ref. [58] has composition $Zr_{0.75}Y_{0.10}Er_{0.05}Th_{0.10}O_{1.925}$. One-phase region has a single phase, cubic $(ZrO_2)_{ss}$; Two-phase region has two cubic zirconia solid solutions with different MO_2 concentration; t–$ZrO_2 = (ZrO_2)_{ss}$ with tetragonal structure; REE = Gd, Y, and other rare-earth elements; $MO_2 = ThO_2$, UO_2, PuO_2 and CeO_2, respectively. The position for the boundary between the one-phase and two-phase regions depends on the type of MO_2 oxides and sintering temperature.

but the data show that a fairly large field has been identified experimentally to make excess weapons plutonium waste forms that consist of only one phase of cubic structure (fluorite type). There is an adjacent field where respective two-phase ceramics have been observed and where both phases are of cubic structure. This field is limited by a two-phase two-component field with phases of different structure. This two-phase field is finally limited by the one-phase field of tetragonal zirconia solid solutions.

6. Conclusions

Ceramics containing simulated excess weapons plutonium waste in solid solution with zirconia can be synthesized using sol–gel and powder methods. Zirconia ceramics with the fluorite-type cubic structure exhibit significant compositional flexibility to incorporate high concentrations of plutonium, neutron absorbers, and impurities contained in plutonium wastes. Ce^{4+} was found to be the best substitute for Pu^{4+} in this system. Synthesis of single-phase zirconia ceramics for Pu wastes is simple. Fabrication technologies of non-plutonium zirconia ceramics are state-of-art. Zirconia solid solutions are known for their high thermal stability and chemical durability. Unlike many other ceramics considered for incorporation of plutonium, irradiation experiments have shown that ZrO_2 is highly resistant to amorphization. ZrO_2 solid solutions are attractive candidates for immobilization and disposal of plutonium wastes.

Acknowledgements

The TEM work was completed in the Microbeam Analysis Facility of the Department of Earth and Planetary Sciences at the University of New Mexico. We thank Donggao Zhao at University of Michigan for XRD analysis of some samples and Nidal Jadalla, Sergey Ushakov, and Abdelessam Abdelouas at University of New Mexico for help with preparation of some sol–gel samples.

References

[1] V.M. Oversby, C.C. MaPheeters, C. Degueldre, J.M. Paratte, J. Nucl. Mater. 245 (1997) 17.
[2] K.E. Sickafus, R.J. Hanrahan Jr., K.N. Mitchell, C.J. Wetteland, D.P. Butt, P. Chodak III, K.B. Ramsey, T.H. Blair, K. Chidester, Hj. Matzke, K. Yasuda, R.A. Verall, N. Yu, Ceram. Bull. 69 (Jan. 1999).
[3] National Academy of Sciences, Management and Disposition of Excess Weapons Plutonium, National Academy Press, Washington DC, 1994, 275 p.; W. Stoll, MRS Bull. March 6 (1998).
[4] W. Stoll, Mater. Res. Soc. Bull. 23 (1998) 6.
[5] D.E. Ferguson, Simple quick processing plant, memo to Floyd Culler, ORNL, USA, 30 (1977).
[6] E. Dzekun, V. Romanovsky, Partitioning installation in Russia is operable, Russian Minatom Monitor, August 19 (1996).
[7] G. Armantrout, L.W. Gray, B. Myers, Plutonium immobilization form evaluation,WM'98 CD-ROM, paper 65–1 (1998).
[8] W. Lutze, R.C. Ewing (Eds.), Radioactive Waste Forms for the Future, North-Holland, New York, 1988.
[9] R.B. Heimann, T.T. Vandergraaf, J. Mater. Sci. Lett. 7 (1988) 583.
[10] F. Vettraino, C. Lombardi, A. Mazzola, Inert matrix nonfertile fuels for plutonium transmutation in PWRs, Plutonium Futures – The Science, Conference Transactions, LANL, 34–34, 1997.
[11] W. Stoll, German Patent No. DE 195 26776 A1, Internat. classification C 01 G 56/00 gehört (1996).
[12] R.C. Ewing, W.J. Weber, W. Lutze, in: E.R. Merz, C.E. Walter (Eds.), Disposal of Weapon Plutonium, Kluwer Academic, Dordrecht, 1996, p. 65.
[13] B.B. Ebbinghaus, R.A. VanKonyneburg, F.J. Ryerson, E.R. Vance, M.W.A. Stewart, A. Jostsons, J.S. Allender, T. Rankin, J. Congdon, in Proc. WM'98 CD-ROM, paper 65–4 (1998).
[14] B.D. Begg, E.R. Vance, S.D. Conradson, J. Alloys Comp. 271 (1998) 221.
[15] W.J. Weber, J.W. Wald, Hj. Matzke, Mater. Lett. 3 (1985) 173.
[16] W.J. Weber, J.W. Wald, Hj. Matzke, J. Nucl. Mater. 138 (1986) 196.
[17] R.C. Ewing, R.F. Haaker, T.J. Headley, P. Hlava, Mater. Res. Soc. Symp. Proc. 6 (1982) 249.
[18] F.W. Clinard Jr., L.W. Hobbs, C.C. Land, D.E. Peterson, D.L. Rohr, R.B. Roof, J. Nucl. Mater. 105 (1982) 248.
[19] F.W. Clinard Jr., Am. Ceram. Soc. Bull. 65 (1986) 1181.
[20] R.C. Ewing, R.F. Headley, J. Nucl. Mater. 119 (1983) 102.
[21] V.M. Oversby, A.E. Ringwood, Rad. Waste Manag. 1 (1981) 289.
[22] W. Sinclair, A.E. Ringwood, Geochem. J. 15 (1981) 229.
[23] R.C. Ewing, B.C. Chakoumakos, G.R. Lumpkin, T. Murakami, Mater. Res. Soc. Bull. 12 (1987) 58.
[24] G.R. Lumpkin, L.M. Wang, Phys. Chem. Miner. 16 (1988) 2.
[25] R.C. Ewing, L.M. Wang, Nucl. Instrum. and Meth. B 65 (1992) 319.
[26] G.R. Lumpkin, R.C. Ewing, Am. Miner. 80 (1995) 732.
[27] S.X. Wang, L.M. Wang, R.C. Ewing, G.S. Was, G.R. Lumpkin, Nucl. Instrum. and Meth. B 148 (1999) 704.
[28] M. Yoshimura, Ceram. Bull. 67 (1988) 1950.
[29] P. Li, I.W. Chen, J.E. Penner-Hahn, J. Am. Ceram. Soc. 77 (1994) 1281.
[30] P. Li, I.W. Chen, J.E. Penner-Hahn, J. Am. Ceram. Soc. 77 (1994) 1289.
[31] P. Li, I.W. Chen, J.E. Penner-Hahn, J. Am. Ceram. Soc. 77 (1993) 118.

[32] D.F. Carroll, J. Am. Ceram. Soc. 46 (1963) 195.
[33] I. Cohen, B.E. Schaner, J. Nucl. Mater. 9 (1963) 18.
[34] F.A. Mumpton, R. Rustum, J. Am. Ceram. Soc. 43 (1960) 237.
[35] J. Katamura, T. Seki, T. Sakamu, J. Phase Equil. 16 (1995) 313.
[36] E. Tani, M. Yoshimura, S. Somiya, J. Am. Ceram. Soc. 66 (1983) 506.
[37] L.L.Y. Chang, M.G. Scroger, B. Philips, J. Am. Ceram. Soc. 50 (1967) 213.
[38] C.E. Curtis, H.G. Sowman, J. Am. Ceram. Soc. 36 (1953) 168.
[39] E. Djurado, C. Roux, A. Hammou, J. Euro. Ceram. Soc. 16 (1996) 767.
[40] H. Asaoka, J. Mater. Sci. 28 (1993) 4660.
[41] P.K. Narwankar, F.F. Lange, C.G. Levi, J. Am. Ceram. Soc. 80 (1997) 1684.
[42] S. Hirano, M. Yoshinaka, K. Hirota, O. Yamaguchi, J. Am. Ceram. Soc. 79 (1996) 171.
[43] P. Barret, P. Berthet, J. Phys. IV 7 (1997) 1141.
[44] Y. Yin, B.B. Argent, J. Phase Equil. 14 (1993) 439.
[45] S.Y. Chen, W.B. Deng, P.Y. Shen, Mater. Sci. Eng. B 22 (1994) 247.
[46] S.B. Qadri, E.F. Skelton, P. Lubitz, N.V. Nguyen, H.R. Khan, Thin Solid Films, vol. 291, 1996.
[47] T. Aoyama, N. Kurata, K. Hirota, O. Yamaguchi, J. Am. Ceram. Soc. 78 (1995) 3163.
[48] G. Fagherazzi, P. Canton, A. Benedetti, F. Pinna, G. Mariotto, E. Zanghellini, J. Mater. Res. 12 (1997) 318.
[49] S. Prietzel, L.J. Gauckler, G. Petzow, Sci. Ceram. 9 (1980) 725.
[50] D.J. Kim, T.Y. Tien, J. Am. Ceram. Soc. 74 (1991) 3061.
[51] H. Naguib, R. Kelly, Radiat. Eff. 25 (1975) 1.
[52] E. Fleischer, M. Norton, M. Zaleski, W. Hertl, C. Carter, J. Mater. Res. 6 (1991) 1905.
[53] N. Yu, K. Sickafus, P. Kodali, M. Nastasi, J, Nucl. Mater. 244 (1997) 266.
[54] K.E. Sickafus, Hj. Matzke, K. Yasuda, P. ChodakIII, R.A. Verrall, P.G. Lucuta, H.R. Andrews, A. Turos, R. Fronknecht, N.P. Baker, Nucl. Instrum. and Meth. B 141 (1998) 358.
[55] C. Degueldre, J.-M. Paratte, Nucl. Tech. 123 (1997) 21.
[56] C. Degueldre, O. Heimgartner, G. Ledergerber, N. Sasajima, K. Hojou, T. Muromura, L. Wang, W. Gong, R. Ewing, Mater. Res. Soc. Proc. Symp. 439 (1997) 625.
[57] N. Yu, R. Devanathan, K.E. Sickafus, M. Nastasi, J. Mater. Res. 12 (1997) 1766.
[58] C. Degueldre, J.M. Paratte, Nucl. Tech. 123 (1998) 21.
[59] W.J. Weber, R.C. Ewing, L.M. Wang, J. Mater. Res. 9 (1994) 688.
[60] W.J. Weber, R.C. Ewing, C.A. Angell, G.W. Arnold, A.N. Cormack, J.M. Delaye, D.L. Griscom, L.W. Hobbs, A. Navrotsky, D.L. Price, A.M. Stoneham, M.C. Weinberg, J. Mater. Res. 12 (1997) 1946.
[61] L.M. Heaman, A.N. Lecheminant, Chem. Geol. 110 (1993) 95.
[62] J.P. Lorand, J.Y. Cottin, Miner. Mag. 51 (1987) 671.
[63] H.R. Naslund, Can. Miner. 25 (1987) 91.
[64] E. Raber, S.E. Haggerty, in: F.R. Boyd, O.A. Meyer Kimberlites (Eds.), Diatremes and Diamonds: Their Geology, Petrology and Geochemistry, AGU, Washington, DC, vol. 1, 1979, p. 229.
[65] S.E. Haggerty, Geochem. Cosmochim Acta 4 (1973) 777.
[66] I.J. Nebrasov, V.V. Ananiev, Dokl. Akad. Nauk SSSR 313 (1990) 947.
[67] C.T. Williams, Miner. Mag. 60 (1996) 639.
[68] C.O. Hutton, Geol. Soc. Am. Bull. 61 (1950) 635.
[69] R.B. Heimann, T.T. Vandergraaf, J. Mater. Sci. Lett. 7 (1988) 583.
[70] D.K. Leung, C.J. Chan, M. Ruhle, F.F. Lange, J. Am. Ceram. Soc. 74 (1991) 2786.
[71] R.C. Ewing, W. Lutze, W.J. Weber, J. Mater. Res. 10 (1995) 243.
[72] A. Rouanet, M. Foex, C.R. Acad. Sci. Ser. C 267 (1968) 875.
[73] W. Lutze, W.L. Gong, R.C. Ewing, in: Proceeding of the International Workshop on Environmental Challenges on Nuclear Disarmament, Cracow, Poland, 8–13, 1998 (in press).
[74] B.E. Burakov, V.G. Khlopin Radium Institute, Russia (personal communication 1999).
[75] W. Dorr, S. Hellmann, G. Mages, J. Nucl. Mater. 140 (1986) 7.
[76] T.D. Chikalla, J. Am. Ceram. Soc. 46 (1963) 326.
[77] M.D. Freshley, H.M. Mattys, in Tech. Rept. HW-76559 (1963).
[78] R.D. Shannon, Acta Crystallogr. A 32 (1976) 751.
[79] J.O.A. Paschoal, H. Kleykamp, F. Thuemmler, Ceramica 30 (1984) 235.
[80] P.E. Evans, J. Am. Ceram. Soc. 43 (1960) 443.
[81] I. Cohen, B.E. Schaner, J. Nucl. Mater. 9 (1963) 18.
[82] K.A. Romberger, C.F. Baes Jr, H.H. Stone, J. Inorg. Nucl. Chem. 29 (1967) 1619.
[83] M. Yahsima, T. Koura, Y. Du, M. Yoshimura, J. Am. Ceram. Soc. 79 (1996) 521.
[84] S. Naz, W. Lutze, R. Busch, A. Prinja, to be published.